https://doi.org/10.5194/egusphere-2026-4167
Preprint. Discussion started: 9 September 2026

Quantitative Modelling of Marine Seismic Hazard Chains: Topology, Core Amplification Nodes, and Implications

Yang Shi[1,2], Chunyu Hu[2], and Zhenguo Zhang[1,2,3]

[1]Department of Earth and Space Sciences, Southern University of Science and Technology, Shenzhen, China
[2]Institute of Risk Analysis, Prediction & Management (Risks-X), Southern University of Science and Technology, Shenzhen, China
[3]Guangdong Provincial Key Laboratory of Geophysical High-resolution Imaging Technology, Southern University of Science and Technology, Shenzhen, China

Correspondence: Zhenguo Zhang (zhangzg@sustech.edu.cn)

Abstract. Earthquakes in marine settings may trigger long chains of secondary hazards. These chains propagate from the seafloor to coastal infrastructure and on to society, yet they have rarely been quantified as a whole. To address this gap, this study proposes a quantitative model of marine seismic hazard chains that combines a catastrophe-dynamics formulation with directed-graph analysis. This network draws on documented secondary hazards from dozens of major tsunamis and includes 39 nodes. This study characterises its topology through degree centrality, network density, centralisation, mean path length, and a layer-resolved net-flow measure. The result is a single-source, dual-hub, multi-sink cascade that is shallow, with most hazards reachable within about two steps. Submarine and coastal earthquakes drive the whole chain, while tsunamis and critical infrastructure failure act as the two high-throughput hubs that amplify and route the flow. Critical network failure is the principal convergence node, where these losses accumulate. The model reveals a monotonic cascade from geological triggers to socioeconomic losses, in which the engineering layer is the gateway through which natural hazards convert into technological failures. A comparison with a mainland earthquake chain at a common taxonomic resolution shows that the two systems share the same four-layer architecture. The mainland earthquake chain exhibits stronger centralisation while the marine tsunami chain presents a more distributed structure. These findings suggest that the controllable engineering hubs, rather than the uncontrollable seismic sources, are the most effective targets for disaster mitigation.

1 Introduction

Disasters rarely act in isolation. A primary hazard often triggers a sequence of secondary events, and the total impact then emerges from the chain as a whole rather than from any single hazard (Gill and Malamud, 2014; Helbing and Kuehnert, 2003). This cascading behaviour is now central to risk assessment, because the indirect losses that accumulate along a chain can exceed the direct loss from the initiating event. Much like a domino effect, such chains spread across natural-geological, engineered-infrastructure, and socioeconomic systems and raise losses gradually. Their secondary impacts extend far past the direct consequences of ground shaking (Gill and Malamud, 2016; Hüning and Brunner, 2026; Pescaroli and Alexander, 2015). Within these cross-system chains, a natural hazard often triggers a technological accident. This coupling is termed Natech,

https://doi.org/10.5194/egusphere-2026-4167
Preprint. Discussion started: 9 September 2026

and it has become a defining feature of coastal seismic risk (Baltzopoulos et al., 2026; Pescaroli and Alexander, 2016). A framework that treats hazards one at a time cannot capture this accumulation. A systems view is therefore needed to track how influence propagates from one event to the next.

Marine seismic events are among the most cascade-prone natural hazards. A single submarine rupture can displace the seafloor, raise a tsunami, and destabilise submarine slopes, and the resulting inundation reaches coastlines that concentrate population, ports, energy supply, and communication networks. The chain then crosses from the natural domain into the engineered one. The 2011 Tohoku earthquake and tsunami provide a typical illustrative example. Natural hazards produced cascading consequences that led to the Fukushima nuclear accident, followed by supply chain disruptions and fluctuations in global financial conditions (Norio et al., 2011). Additional disaster cases further clarify this pattern. The 2018 Palu catastrophe showed that submarine landslides can dominate tsunami generation inside narrow bay environments (Somphong et al., 2022), and the 2024 Noto earthquake again coupled seafloor failure to coastal damage (Masuda et al., 2024; Park et al., 2026; Yuhi et al., 2024). In each case, this Natech coupling acted as a recurrent amplifier of total loss.

Hazard-chain research has developed a diverse methodological toolbox to study such cascades. Pescaroli and colleagues built a theoretical framework for cascading disasters and cascading effects, emphasising the central role of critical-infrastructure interdependency along the propagation path (Pescaroli and Alexander, 2015, 2016, 2018). Bayesian networks quantify causal propagation under uncertainty in seismic hazard chains (Han et al., 2019a, b; Kabir et al., 2019; Wang et al., 2013). Disaster-system simulations, such as HLA co-simulation and CIA-DISM models, reproduce the propagation mechanisms of hazard chains and their consequences (Wang et al., 2022; Yu et al., 2014). Remote sensing and geographic information systems track the spatial patterns of seismic hazard chains and inform emergency-response decisions (Fan et al., 2022; Xu et al., 2014a). Interdisciplinary frameworks integrate geoscience, engineering, and the social sciences to identify the cross-system interdependencies of disasters (Alexander and Pescaroli, 2019; Shi et al., 2020). Statistical and engineering-geology methods assess chain-driving factors and specific failures, such as structural damage, landslides, slope instability, and dam breaching (Chen et al., 2022; Fan et al., 2012; Tacconi Stefanelli et al., 2016; Xu et al., 2014b; Yang et al., 2023). Graphs provide a natural language for these chains, in which hazards become vertices and triggering relationships become directed edges, so that the tools of network science can quantify the structure of a cascade and locate the nodes that matter most (Gill and Malamud, 2014; Mignan et al., 2022a; Rocha et al., 2018). Centrality measures distinguish the hazards that initiate many chains from those that absorb them, while aggregate measures, such as density and centralisation, summarise how concentrated or distributed the cascade is. Building on this idea, catastrophe-dynamics formulations express the couplings between events as a transition matrix and accumulate them over successive steps into a single interaction operator (Mignan and Wang, 2020). This makes both the number of interactions and the strength of their propagation computable.

Despite this progress, marine seismic hazard chains have not been characterised systematically as networks, and several questions therefore remain open. It is not clear which nodes amplify a marine seismic cascade, where in the chain natural hazards convert into technological failures, or how the marine case differs from the better-studied mainland one. This study addresses these questions. It constructs a directed hazard network for marine seismic chains from the documented record of major tsunamis, using a refined peril taxonomy organised into trigger, process, and consequence layers. This study first

https://doi.org/10.5194/egusphere-2026-4167
Preprint. Discussion started: 9 September 2026

characterises the topology of the network and identifies its amplifying hubs, then uses a layer-resolved net-flow measure to locate the Natech gateway within the cascade. Next, it compares the marine network with a mainland earthquake network at a common taxonomic resolution, so that genuine structural differences are separated from artefacts of resolution. The analysis gives a compact description of how marine seismic risk propagates, and points to the hubs where mitigation has the greatest leverage.

2 Method

2.1 Cascading chain modelling approach

Cascading disasters propagate as sequences of interacting events, and characterising them requires a framework that tracks how influence spreads over time. This study therefore adopts catastrophe dynamics, a systems-theoretic formulation that quantifies the direct and indirect couplings which accumulate during disaster evolution (Helbing and Kuehnert, 2003; Mignan and Wang, 2020).

Let $S = \{1, 2, \ldots, n\}$ denote the set of non-terminal disaster states and let $n+1$ denote an absorbing terminal state representing the cessation of further propagation, so that the full state space is $S \cup \{n+1\}$. The model in this study rests on three assumptions. First, the pairwise interactions between events are mutually independent (no higher-order/synergistic coupling). Second, only pairwise interactions between disasters enter the analysis. Third, the system follows Markovian dynamics, so that its future evolution depends only on the current state and not on the path taken to reach it. Under these assumptions, a continuous-time Markov process describes how the disaster-event probabilities evolve. Using the row-vector convention, let $\boldsymbol{\pi}(t)$ denote the probability distribution over the full state space at time t. Its dynamics are governed by

$$\frac{\mathrm{d}\boldsymbol{\pi}(t)}{\mathrm{d}t} = \boldsymbol{\pi}(t)\,\mathbf{Q}, \tag{1}$$

where $\mathbf{Q} = (q_{ij})$ is the transition-rate generator. For $i \neq j$, $q_{ij} \geq 0$ denotes the instantaneous transition rate from disaster event i to disaster event j, while the diagonal entries satisfy

$$q_{ii} = -\sum_{j \neq i} q_{ij}, \tag{2}$$

so that each row of $\mathbf{Q}$ sums to zero:

$$\sum_{j} q_{ij} = 0. \tag{3}$$

The transition probability matrix over an interaction interval τ is then given by the matrix exponential

$$\mathbf{P}(\tau) = \exp(\mathbf{Q}\tau), \tag{4}$$

with entry

$$p_{ij}(\tau) = \Pr\{X(t+\tau) = j \mid X(t) = i\}. \tag{5}$$

https://doi.org/10.5194/egusphere-2026-4167
Preprint. Discussion started: 9 September 2026

Thus, $p_{ij}(\tau)$ represents the conditional probability that a chain currently in state i reaches state j after an interval τ. Here, τ is interpreted as a pseudo-time index measuring the number of interaction steps along the disaster chain, with the degenerate case $\tau = 0$ excluded from cascade propagation. The propagation horizon is set to $\tau = 10$, following Mignan and Wang (2020). Their work shows that emergent cascades, represented by the cumulative interaction matrix $\mathbf{M}$ defined below, have stabilised by this step. The shallow network studied here converges likewise, so the reported topology does not depend on this choice.

Evaluating the propagator at one interaction step gives the single-step transition matrix

$$\mathbf{P}(1) = \exp(\mathbf{Q}). \tag{6}$$

The non-terminal submatrix of $\mathbf{P}(1)$ is denoted by

$$\mathbf{A} = \left[p_{ij}(1)\right]_{i,j=1}^{n}. \tag{7}$$

The entry a_{ij} therefore denotes the one-step conditional probability that disaster event i triggers, or is followed by, disaster event j. In graph-theoretic terms, $\mathbf{A}$ defines a weighted directed network of disaster couplings, where nodes represent disaster events and edge weights represent transition probabilities (Gill and Malamud, 2014; Mignan et al., 2022a; Rocha et al., 2018).

Because the absorbing terminal state is omitted from the displayed matrix $\mathbf{A}$, this matrix is generally substochastic rather than stochastic:

$$\sum_{j=1}^{n} a_{ij} \leq 1. \tag{8}$$

The residual probability

$$a_{i,n+1} = 1 - \sum_{j=1}^{n} a_{ij} \tag{9}$$

is assigned to the absorbing terminal state. This construction preserves probability conservation while allowing the modelled cascade to end after any interaction step.

A single application of $\mathbf{A}$ advances the hazard chain by one step. Longer cascades are represented by successive matrix products. Specifically, $\mathbf{A}^2$ gives all two-step propagation probabilities, $\mathbf{A}^3$ gives all three-step propagation probabilities, and so forth. Therefore, the total interaction matrix is defined as

$$\mathbf{M} = \sum_{\tau=1}^{\infty} \mathbf{A}^{\tau} = \mathbf{A} + \mathbf{A}^2 + \mathbf{A}^3 + \cdots. \tag{10}$$

Provided that the spectral radius satisfies

$$\rho(\mathbf{A}) < 1, \tag{11}$$

this series converges and can be written in closed form as

$$\mathbf{M} = \mathbf{A}(\mathbf{I} - \mathbf{A})^{-1} = (\mathbf{I} - \mathbf{A})^{-1} - \mathbf{I}. \tag{12}$$

https://doi.org/10.5194/egusphere-2026-4167
Preprint. Discussion started: 9 September 2026

The convergence condition is naturally satisfied when the cascade has a nonzero probability of eventual absorption, meaning that disaster chains terminate with probability one.

The element $(\mathbf{A}^{\tau})_{ij}$ aggregates the probabilities of all paths of length τ that start from disaster event i and reach disaster event j. Explicitly,

$$(\mathbf{A}^{\tau})_{ij} = \sum_{k_1,\ldots,k_{\tau-1}} a_{ik_1}\, a_{k_1k_2} \cdots a_{k_{\tau-1}j}. \tag{13}$$

Accordingly, the entry m_{ij} of $\mathbf{M}$ represents the cumulative propagation influence from event i to event j over all possible chain lengths. It includes both direct effects, captured by $\mathbf{A}$, and indirect effects, captured by higher-order powers of $\mathbf{A}$. In this sense, $\mathbf{M}$ characterises the overall spatial and systemic reach of cascading disasters, including multi-step propagation routes and feedback loops through which disasters may amplify one another's impacts (Mignan et al., 2022b). The summation across all path lengths further captures the long-tailed characteristics of cascading effects. Even with a low direct triggering probability, cumulative indirect propagation pathways can collectively produce substantial overall risk.

The empirical analysis in this study uses the structure of these operators, not their calibrated weights. The documented record specifies which couplings occur, but not their transition rates. The reported metrics are therefore computed on the support of $\mathbf{A}$ and $\mathbf{M}$, that is, on the binary directed graph of documented couplings and its reachability. Degree, centralisation, density, and layer net flow follow from the edge set of $\mathbf{A}$, whereas the cascade-reach analysis of the Discussion follows from the reachability pattern of $\mathbf{M}$, namely from whether $m_{ij} > 0$. This structural reading is deliberately conservative, because it does not depend on any particular choice of transition rate. Attaching empirical triggering probabilities and time delays to the edges is left to future work, consistent with the binary-edge limitation noted in the Discussion.

2.2 Peril taxonomy

To better represent the hazard chains triggered by tsunamis, this study refines the peril nodes. The refinement follows the framework in the Mignan (2024) textbook. Table 1 summarises the resulting taxonomy. The classification follows the theoretical structure of a hazard chain, which includes an initial triggering hazard, an intermediate process hazard, and the consequent socioeconomic outcomes. Table 1 classifies the relevant hazards along this structure.

2.3 Graphs characterise hazard chains

A graph offers a natural representation of hazard chains. The vertices represent entities such as earthquakes or landslides, and the edges encode the relationships between them, for example the triggering link from an earthquake to a landslide. In graph theory, the centrality of a vertex quantifies how well it connects to the others, and so serves as a primary indicator of the vertex's importance in the network. In directed graphs, this metric comprises two components. In-degree centrality quantifies edges incoming to a given vertex, whereas out-degree centrality quantifies edges outgoing from the vertex to other nodes. A vertex of higher centrality occupies a more pivotal position and exerts a stronger influence. On this basis, this study applies the graph framework to a dataset of several hundred earthquake-induced secondary hazard chains, which were generated by dozens of major tsunamis worldwide over recent decades and span several representative chain types.

https://doi.org/10.5194/egusphere-2026-4167
Preprint. Discussion started: 9 September 2026

Table 1. Peril taxonomy used to define the nodes of the marine seismic hazard network.

Peril / Code	Notes
Trigger layer	
Submarine Earthquake / SEQ	Subduction-zone / seafloor fault rupture, vertical seafloor displacement (primary physical trigger of tsunamis)
Coastal Earthquake / EQ	Ground shaking, fault rupture, ground displacement
Aftershock / AS	Continued cascade triggering after the mainshock; may re-induce submarine landslides
Volcanic Eruption / VE	May trigger volcanic tsunamis
Process layer — Natural	
Submarine Landslide / SLS	Seafloor instability / turbidity currents
Coastal Landslide / CLS	Coastal cliff/slope instability; landslides entering the sea may generate secondary waves
Landslide / LS	Co-seismic slope failure (generic)
Rockfall / RO	Rockfall from coastal cliffs
Lake Burst / LB	Lake / reservoir outburst
Snow Avalanche / SA	—
Liquefaction / LI	Liquefaction of coastal soft soil / reclaimed port fill (a leading cause of port and seawall failure)
Ground Uplift / GU	—
Subsidence / SUB	Subsidence (a direct hazard to coastal cities)
Methane Blowout / MB	—
Tsunami / TS	Near-field / far-field tsunamis, including trans-oceanic propagation
Coastal Flooding / CFL	Seawater intrusion, estuarine compound flooding, astronomical-tide superposition
Fluvial Flood / FF	Compound floods superimposed on coastal flooding
Marine Ecosystem Damage / MED	Coral-reef bleaching/die-off, mangrove destruction, fishery collapse, red tides
Water Pollution / WP	Seawater pollution, freshwater salinization, oil-spill dispersion
Water Dilemma / WD	Drinking-water shortage, channel blockage, saltwater intrusion
Disease / DI	Post-disaster cholera, dengue, and other epidemic outbreaks
Flora and Fauna / FA	Loss of fishery resources; destruction of coastal vegetation
Process layer — Engineering	
Port / Harbour Failure / PHF	Wharf structural damage, gantry-crane collapse, vessel damage or sinking
Seawall / Dike Failure / SDF	Breakwater failure, revetment damage, sea-reclamation works failure
Subsea Pipeline Failure / SPF	Damage to subsea oil/gas pipelines, water-supply mains, outfalls
Subsea Cable Failure / SCF	$\sim$95 % of global international data relies on submarine cables; cross-border cascading communication outage
Nuclear Facility Accident / NFA	Fukushima-type cascade: coastal nuclear-plant cooling / spent-fuel-pool failure
Fire / FI	Refinery, oil-tank, LNG, and vessel fires
Explosion / EX	LNG terminals, oil/gas facilities, chemical storage
Critical Infrastructure Failure / CF	Coastal power plants, desalination plants, coastal airports, petrochemical storage, building collapse/damage, fishing vessels
Critical Network Failure / NF	Power grid / transport / communication / water-supply / gas networks (incl. submarine cables, port-shipping networks)
Consequence layer	
Maritime Transport Disruption / MTD	Channel blockage, port closure, cross-border supply-chain disruption
Business Interruption / BI	Industry / fishery / tourism / cross-border trade / commerce
Economic Crisis / EC	Regional recession, insurance-payout crisis, exchange-rate and reinsurance contagion
Physical and Psychological Trauma / PP	Death, drowning, missing persons, trauma, bereaved families
Healthcare Degradation / HD	Hospital overload, supply shortages, public-health control failure
Insufficient Rescue / IR	Difficult maritime search-and-rescue, isolated-island rescue, cross-border coordination barriers, rescue interruption
Social Unrest / SU	Riots, strikes, looting, terrorist attacks, civil disorder
Culture Perils / CP	Coastal heritage sites, fishing-village / religious-culture damage, examination / school disruption

https://doi.org/10.5194/egusphere-2026-4167
Preprint. Discussion started: 9 September 2026

2.4 Metrics definitions

This study characterises and compares the two disaster-chain networks with four metrics. Each metric is computed on a directed graph $G = (V, E)$ with $N = |V|$ nodes and E edges.

(1) *Network density* measures how many of the possible links are realised,

$$\text{density} = \frac{E}{N(N-1)}, \tag{14}$$

where N is the number of nodes and E the number of edges. It ranges from 0 (no links) to 1 (every node points to every other). Higher values indicate more richly interconnected hazards.

(2) *Out-degree centralisation* quantifies how strongly the out-edges concentrate in a single node,

$$C_{\text{out}} = \frac{\sum_i (d_{\max}^{\text{out}} - d_i^{\text{out}})}{(N-1)^2}, \tag{15}$$

where d_i^{out} is the out-degree of node i and $d_{\max}^{\text{out}}$ the maximum. It ranges from 0, when all nodes trigger equally, to 1 for a perfect star dominated by one source. This study computes the in-degree centralisation C_{in} analogously, to gauge convergence on the consequence side.

(3) *Mean path length* is the average number of edges on the shortest directed path over all ordered pairs of reachable nodes. It reports how many steps a shock typically travels between hazards, with unreachable pairs excluded.

(4) *Layer net flow* describes the role of each of the four layers. For a layer l, it is defined as

$$\text{net}_l = \sum_{i \in l} d_i^{\text{out}} - \sum_{i \in l} d_i^{\text{in}}, \tag{16}$$

normalised by $|E|$ to allow comparison across networks. A positive value marks a net source that drives the cascade and a negative value a net sink that absorbs it. Because within-layer edges contribute equally to both terms, net_l depends only on cross-layer flow.

3 Quantitative modelling results

3.1 Node characteristics of marine seismic hazard chains

The marine disaster-chain network comprises 39 nodes and 152 directed edges (Fig. 1a and b). Its degree distribution is heavy-tailed, and it forms a single-source, dual-hub, multi-sink topology. The out-degree distribution first identifies two pure first-order triggers, submarine earthquakes (SEQ; out-degree 29, in-degree 0) and coastal earthquakes (EQ; out-degree 13, in-degree 0), both of which initiate cascades yet are triggered by no other hazard. Submarine earthquakes alone account for roughly three-quarters of all hazard types. Downstream hazard amplification relies on two core hubs. Tsunamis (TS) lead the natural-process branch, critical infrastructure failure (CF) dominates the engineering branch, and together they expand a single seismic source into dozens of secondary chains. The in-degree distribution tells the opposite story. Here critical infrastructure

https://doi.org/10.5194/egusphere-2026-4167
Preprint. Discussion started: 9 September 2026

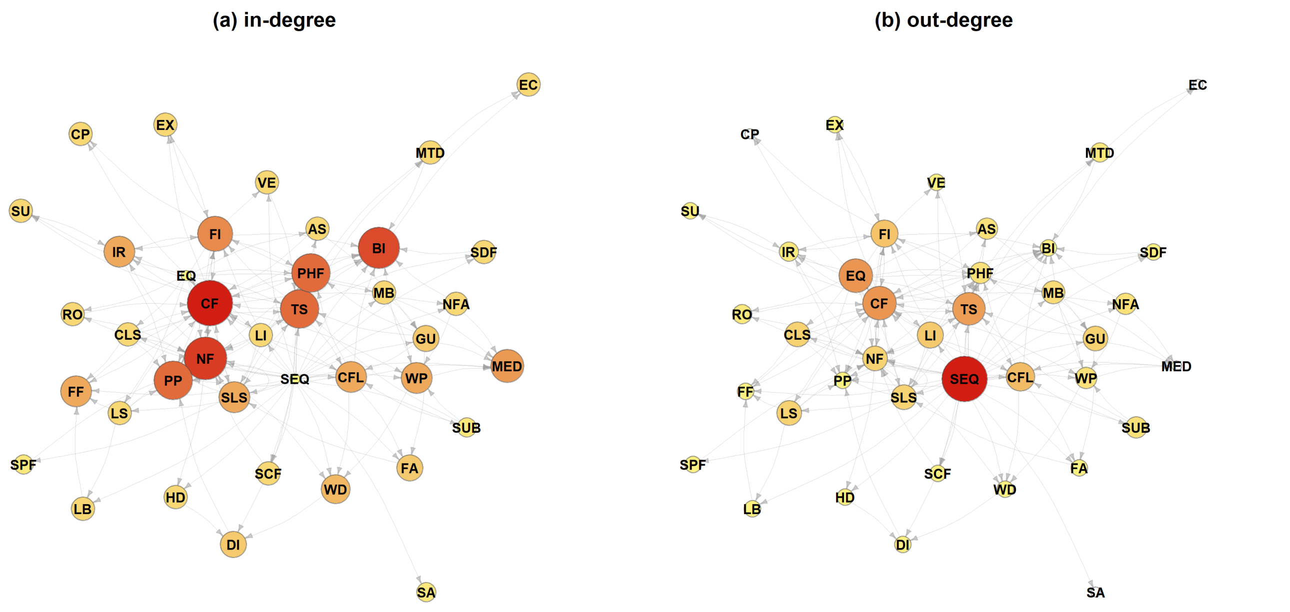

Figure 1. Disaster-chain networks of marine seismic hazards: (a) in-degree centrality; (b) out-degree centrality. Warmer colours indicate higher in/out-degree centrality. An interactive version is available at https://hazardchain.github.io/NHESS-marine-seismic-hazard-chains-code-data/.

failure (CF; in-degree 14) and critical network failure (NF; in-degree 12) emerge as the principal convergence nodes, where a broad range of natural hazards accumulate before cascading into terminal consequences such as business interruption (BI), physical and psychological trauma (PP), and economic crisis (EC). Critical infrastructure failure carries a high in-degree and a high out-degree at the same time. It works as the gateway that turns natural hazards into socioeconomic losses, a pronounced signature of Natech (natural-hazard-triggered technological disaster) cross-layer coupling. Critical network failure, in contrast, combines a high in-degree with a modest out-degree, and is thus the principal convergence node where these losses accumulate rather than a hub. These results carry a clear implication. The most effective points for disrupting the cascade are not the inherently uncontrollable seismic sources, but the amplifying hub, namely critical infrastructure failure, together with the critical-network convergence node. Table 2 summarises the network's core nodes.

3.2 Layer aggregation reveals a four-stage cascade

This study aggregates the 39 distinct hazard nodes into four hierarchical tiers: triggers, natural processes, engineering processes, and consequences. This simplification reveals the core topological structure of the disaster cascade. Table 3 lists the aggregated flows across these layers, where the net flow of each layer equals its total out-degree minus its total in-degree. The aggregated meta-network forms a monotonic energy waterfall. The net flow falls steadily down the hierarchy: $+42$ at the trigger layer, $+1$ at the natural-process layer, -16 at the engineering-process layer, and -27 at the consequence layer.

https://doi.org/10.5194/egusphere-2026-4167
Preprint. Discussion started: 9 September 2026

Table 2. Most important nodes in our modelling.

Code	Hazard	Layer	In-degree	Out-degree	Net flow	Role
SEQ	Submarine earthquake	Trigger	0	29	+29	Primary source
EQ	Coastal earthquake	Trigger	0	13	+13	Primary source
TS	Tsunami	Process–Natural	9	12	+3	Relay hub
CFL	Coastal flooding	Process–Natural	5	8	+3	Relay hub
CF	Critical infrastructure failure	Process–Engineering	14	13	−1	Relay hub
NF	Critical network failure	Process–Engineering	12	5	−7	Sink
PHF	Port/harbour failure	Process–Engineering	9	3	−6	Sink
FI	Fire	Process–Engineering	7	7	0	Relay hub
BI	Business interruption	Consequence	11	1	−10	Terminal sink
PP	Physical and psych. trauma	Consequence	9	1	−8	Terminal sink

Notes: [1] Nodes are included if their in-degree or out-degree ≥ 7, corresponding to the upper quartile of the degree distribution (39 nodes total). [2] Net flow = out-degree − in-degree; positive values indicate source-leaning (driver) nodes and negative values indicate sink-leaning (consequence) nodes. [3] Primary source: in-degree = 0; initiates cascades, never induced. [4] Relay hub: high in- and out-degree with out-degree comparable to in-degree (small |net flow|); receives and re-propagates, i.e. amplifies the cascade. [5] Sink: out-degree markedly below in-degree (strongly negative net flow); absorbs more than it re-propagates. "Terminal sink" marks consequence-layer endpoints (out-degree ≈ 1, no further propagation).

These values together tell a clear story. The trigger layer dominates the entire cascading chain. It outputs 46 edges while receiving merely 4 edges, thereby providing nearly all the initial driving force for hazard propagation. The natural-process layer stays close to balance, sending 63 edges and receiving 62. It thus acts as a conduit rather than a reservoir, translating seismic energy into tsunamis, coastal flooding, and landslides before passing these secondary hazards downstream. The engineering-process layer marks a turning point. This layer exhibits a substantial net sink of −16. Various natural hazards converge here and trigger failures of critical infrastructures and networks. This layer thus mediates the transition from natural hazards to technological disasters and marks the primary location of Natech cross-coupling. Finally, the consequence layer ends the cascade as the terminal sink, at −27, where the chain settles into socioeconomic losses such as business interruption, physical and psychological trauma, and economic crisis, and propagates no further. Taken together, these results reduce an apparently complex hazard network to a simple four-stage cascade, in which energy flows monotonically from geological triggers towards societal outcomes. The engineering-process layer occupies the pivotal position. It links natural-hazard generation to social and economic damage, and marks the point where the cascade crosses from the natural to the technological domain. The greatest leverage for intervention, however, lies not with the layer as a whole, but with the high-throughput hub node that carries the cascade into and through this stage, namely critical infrastructure failure (Sect. 3.1).

3.3 A comparison of mainland and marine earthquake hazard chains

To ensure a fair comparison, this study reduces both networks to the same 15 aggregated hazard classes, with the full node-to-class aggregation given in Table A1. Duplicate edges and self-loops are removed before any metric is evaluated. At this

https://doi.org/10.5194/egusphere-2026-4167
Preprint. Discussion started: 9 September 2026

Table 3. Aggregated degree flows across the four hazard layers.

Layer	Nodes	Out-flow*	In-flow	Net flow	Net flow (%)	Cascade stage
Trigger	4	46	4	+42	+27.6 %	Source (driver)
Natural process	18	63	62	+1	+0.7 %	Conduit
Engineering process	9	35	51	−16	−10.5 %	Natech gateway
Consequence	8	8	35	−27	−17.8 %	Terminal sink
Total	39	152	152	0	0 %	—

* Out-flow and in-flow are the total out-degree and in-degree summed over the member nodes of each layer; net flow = out-flow − in-flow, reported both as a raw count and as a percentage of the 152 edges. A positive value marks a source-leaning layer that drives the cascade and a negative value a sink-leaning layer that absorbs it. Net flow falls monotonically down the hierarchy, tracing the four-stage cascade from geological triggers to socioeconomic losses.

common resolution, the marine and mainland earthquake disaster chains share the same four-layer cascade architecture (Fig. 2 and Table 4). The seismic trigger supplies almost all of the initiating drive, the natural-process layer stays close to balance and conducts the flow onward, the engineering layer carries it further, and the consequence layer absorbs the full impact. Both chains are shallow, with mean path lengths of about 1.90 and 1.86 steps, so a seismic shock reaches most other hazards within one or two hops — a pattern typical of a single-source radial cascade. The two chains differ in degree, not in kind. The mainland chain depends heavily on a single seismic source. Its out-degree centralisation reaches 0.832, and it routes a net inflow of about 45 % of all edges into the consequence layer, which gives it a concentrated, consequence-directed profile. The marine chain behaves differently. This hazard can propagate via multiple secondary channels including tsunamis and submarine landslides. With an out-degree centralisation of merely 0.551 and a high network density of 0.271, risk flows circulate horizontally among intermediate layers before eventually terminating. The net flow sign of the engineering layer varies across different classification resolutions. Consistent with the findings in Sect. 3.2, such variation originates entirely from network aggregation. The integration of numerous discrete natural hazards linked to engineering nodes eliminates redundant cross-layer connections, enabling the engineering layer to present as a net sink under fine-resolution configurations. The two findings are therefore compatible, and each holds at its own resolution.

3.4 Robustness and sampling sufficiency

The network follows from the documented cascade record through expert encoding, so the study in this section examines whether its topology and the conclusions it supports reflect a robust structure rather than artefacts of individual one-off links (Fig. 3). The 366 documented chains cluster under 58 source events (tsunamis), and every check therefore treats the event as the sampling unit and resamples at the event level (Efron and Tibshirani, 1993; Huang, 2018). All checks target the edge set, since the reported degree-based metrics do not depend on the coupling weight.

A first check raises the inclusion threshold from one documented event to two and then three independent events, which progressively removes low-frequency links. The analysis rests on four qualitative conclusions. Submarine and coastal earthquakes

https://doi.org/10.5194/egusphere-2026-4167
Preprint. Discussion started: 9 September 2026

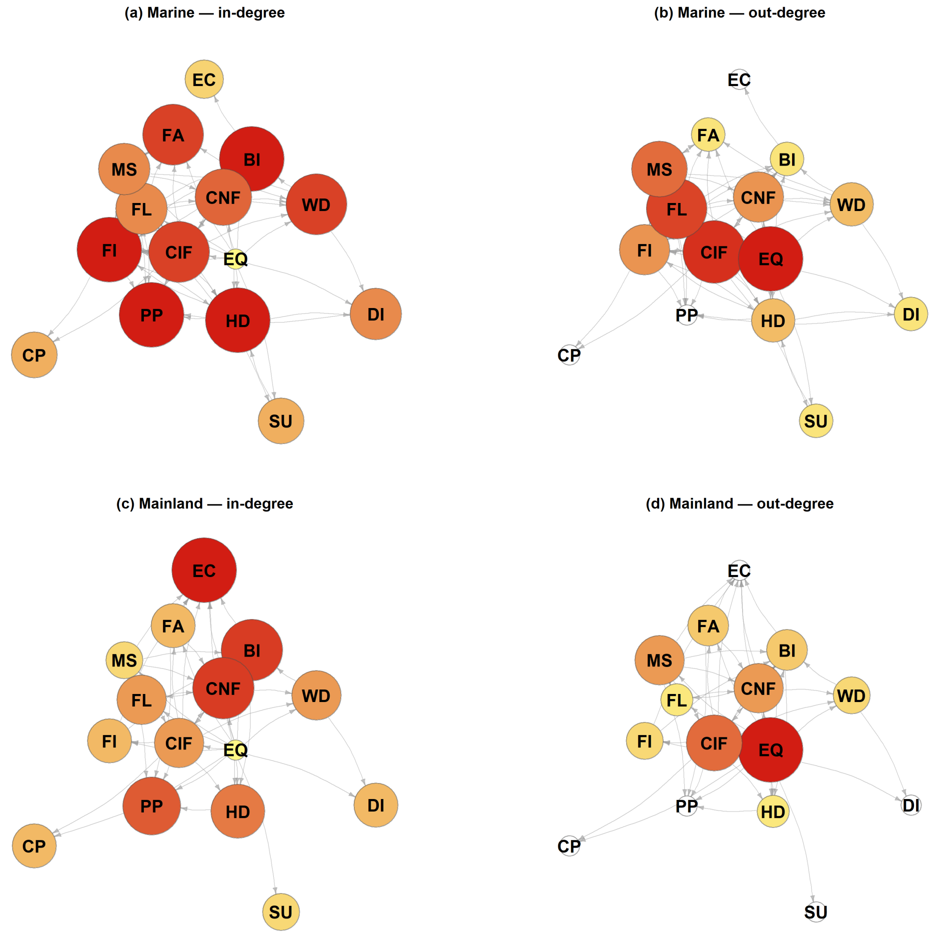

Figure 2. Comparison of the marine and mainland earthquake disaster-chain networks at a unified resolution of 15 aggregated hazard classes. Within each network the same class occupies the same position (panels a,b share one layout and panels c,d share another), so in- and out-degree can be compared directly across panels of the same network. Node colour and node size both encode degree on a yellow-to-red scale, with larger and redder nodes denoting higher degree. In the out-degree panels, pure sink nodes with zero out-degree are drawn in white. Labels are class abbreviations (EQ, earthquake/trigger; MS, mass slide; FL, flood; CIF, critical infrastructure failure; CNF, critical network failure; FI, fire; WD, water dilemma; FA, flora and fauna; BI, business interruption; HD, healthcare degradation; EC, economic crisis; DI, disease; PP, physical and psychological trauma; CP, culture perils; SU, social unrest). (a, b) Marine chain coloured by in-degree and out-degree. (c, d) Mainland chain coloured by in-degree and out-degree. An interactive version is available at https://hazardchain.github.io/NHESS-marine-seismic-hazard-chains-code-data/.

are the only pure sources (C1), the submarine earthquake forms the dominant out-hub and critical infrastructure failure the dominant in-hub (C2), critical network failure acts as a convergence node (C3), and the layer net flow decreases monotonically from trigger to consequence (C4). All four persist at the ≥ 1 and ≥ 2 thresholds, and only the convergence character of critical

https://doi.org/10.5194/egusphere-2026-4167
Preprint. Discussion started: 9 September 2026

Table 4. Comparison between marine and mainland seismic hazard networks.

Metric	Marine (15 classes)	Mainland	Higher value indicates
Nodes / edges	15 / 57	15 / 47	—
Network density	0.271	0.224	More hazards are interconnected
Out-degree centralisation	0.551	0.832	Triggering concentrated in one source
In-degree centralisation	0.168	0.296	Consequences converge more sharply
Max out-degree	11	14	A more dominant single trigger
Pure sources / sinks	1 / 3	1 / 5	More terminal endpoints
Mean path length	1.90	1.86	Almost equal
Net flow* — Trigger layer	$+19.3\,\%$	$+29.8\,\%$	Stronger source layer
Net flow — Natural layer	$+3.5\,\%$	$+2.1\,\%$	(near balance = conduit)
Net flow — Engineering layer	$+8.8\,\%$	$+12.8\,\%$	Forwarding
Net flow — Consequence layer	$-31.6\,\%$	$-44.7\,\%$	Sharper terminal absorption

* Net flow is reported as a percentage of total edges; positive values mark source-leaning layers and negative values mark sink-leaning layers. All metrics are computed in R.

network failure (C3) weakens once the network reduces to its ≥ 3 core of 46 edges, which shows that mid-frequency rather than the highest-frequency links support this node.

A second check applies an event-level cluster bootstrap that resamples the 58 source events with replacement ($B = 1000$) and rebuilds the network from every chain of those events. Core topological metrics exhibit strong robustness across resampling trials. The submarine-earthquake out-degree averages 24.1 across resamples (95 % interval $[17, 29]$) and the critical-infrastructure-failure in-degree averages 12.4 ($[10, 14]$). The four qualitative conclusions C1–C4 hold in 88–100 % of resamples (Fig. 3b). Resampling events rather than individual chains avoids pseudo-replication and yields deliberately conservative intervals.

A third check assesses the sampling sufficiency and completeness of the record (Casas et al., 2018). The edge-accumulation curve (Fig. 3a) rises steeply and then flattens without fully saturating, so rare pathways would continue to accrue with additional events. A five-fold analysis of out-of-sample edge coverage confirms this asymmetry. Across all links, only $\sim$74 % of those in a held-out fold of events already appear in the network that the remaining events build (mean over 200 random five-fold splits), whereas that same network recovers $\sim$98 % of the higher-frequency core links that appear in at least two events. Accordingly, the core network backbone supporting all research conclusions is fundamentally complete and reproducible. Data incompleteness only affects the long-tail rare links of individual disaster events and exerts no influence on network topology. These validation checks demonstrate that the identified cascading structure reflects inherent characteristics of empirical disaster chain records, rather than deriving from artificial encoding biases. Although rare long-tail links slightly affect quantitative edge counts, they do not alter any qualitative findings of this study.

https://doi.org/10.5194/egusphere-2026-4167
Preprint. Discussion started: 9 September 2026

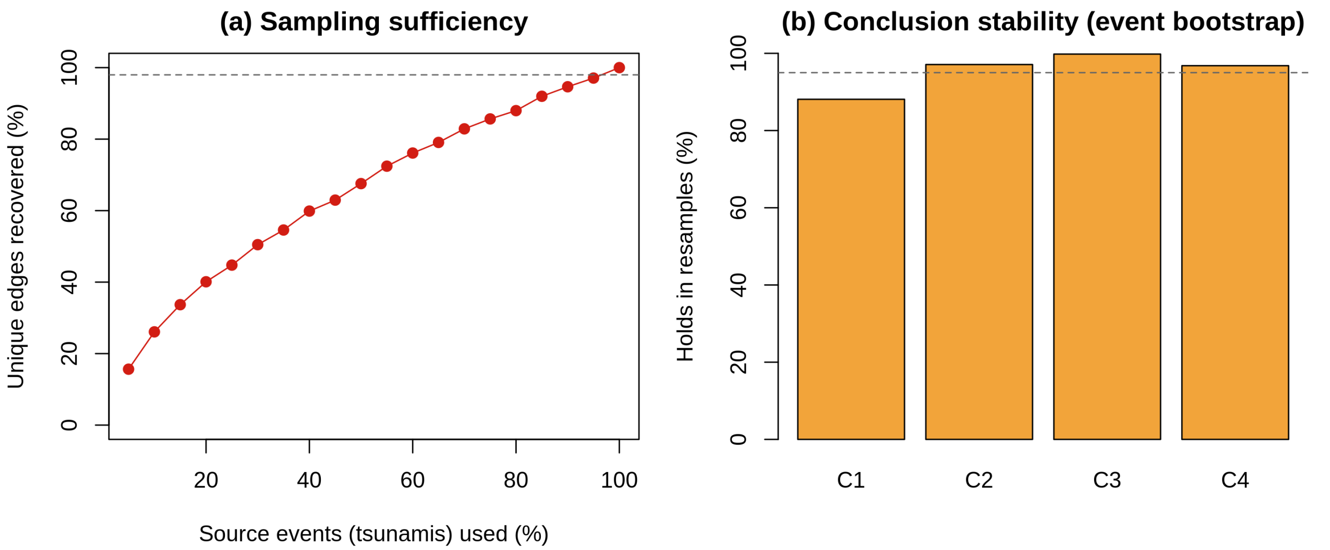

Figure 3. Robustness and sampling sufficiency of the marine hazard network; all resampling is at the level of the 58 source events (tsunamis). (a) Edge-accumulation curve: unique directed links recovered as a function of the fraction of source events used (mean of 200 random orderings); the dashed line marks the out-of-sample coverage of the high-frequency core links (documented in ≥ 2 events), recovered at $\sim$98 % (mean over 200 random five-fold splits). (b) Fraction of $B = 1000$ event-level bootstrap resamples in which each qualitative conclusion holds (C1, pure sources; C2, dominant hubs; C3, network-failure convergence node; C4, monotonic four-layer cascade); the dashed line marks 95 %.

3.5 Out-of-sample hindcast

The network and its analysis draw on the same record, so an independent test is needed to show that the structure predicts rather than merely describes. Three major submarine-earthquake tsunamis that lie outside the compilation, the 2004 Indian Ocean, the 1960 Valdivia and the 2018 Palu events, provide that test, with every cascade link documented and individually sourced. Encoding these events and comparing them against the network shows that 40 of their 54 documented couplings, that is 74 %, already exist in the paper's network (Fig. 4 and Table 5). The 14 remaining couplings connect perils that the taxonomy already contains, so the three events add no new hazard type. Merging them into the record leaves every reported conclusion intact. Pure hazard sources remain exclusively submarine and coastal earthquakes, with submarine earthquakes retaining the dominant out-hub status and critical infrastructure failure remaining the primary in-hub. Meanwhile, critical network failure consistently serves as a convergence node, and the four-layer net flow maintains a monotonic decreasing trend from the trigger layer to the consequence layer (Table 6). Node importance is equally stable, with a Spearman rank correlation of 0.97 for out-degree and 0.96 for in-degree between the original and the augmented network. The conclusions therefore describe the documented cascade itself rather than the particular events that built it. The 14 novel couplings are the rare, event-specific links that Sect. 3.4 isolates as the sensitive tail, so the new events enrich that tail without disturbing the backbone.

https://doi.org/10.5194/egusphere-2026-4167
Preprint. Discussion started: 9 September 2026

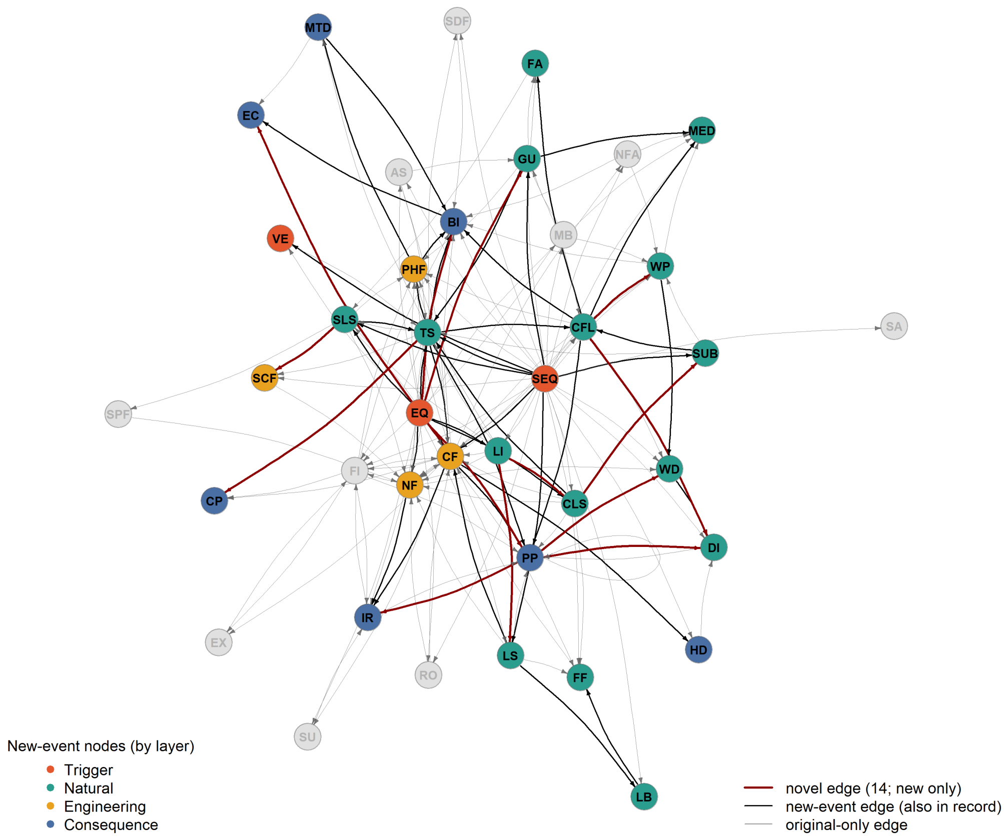

Figure 4. The three independent events (2004 Indian Ocean, 1960 Valdivia and 2018 Palu) overlaid on the marine network. Nodes touched by the new events are coloured by layer and their labels are black. The 14 couplings absent from the original record are drawn in dark red, the remaining new-event couplings in black, and every node, edge and label that belongs only to the original network in grey. The new events reconfirm the existing sources, hubs and layer structure and add only peripheral, mostly consequence-side links. An interactive version is available at https://hazardchain.github.io/NHESS-marine-seismic-hazard-chains-code-data/.

Table 5. Directed-edge coverage of the three independent events by the marine network.

Event	Links	In network	Coverage
1960 Valdivia	17	16	94 %
2004 Indian Ocean	26	19	73 %
2018 Palu	29	22	76 %
All three combined	54	40	74 %

https://doi.org/10.5194/egusphere-2026-4167
Preprint. Discussion started: 9 September 2026

Table 6. The four qualitative conclusions before and after merging the three independent events into the record.

Quantity	**Original (58 events)**	**Augmented (61 events)**
Nodes / edges	39 / 152	39 / 166
Pure sources	SEQ, EQ	SEQ, EQ
Dominant out-hub / in-hub	SEQ / CF	SEQ / CF
Critical network failure, in / out	12 / 5	12 / 5
Layer net flow (T/N/E/C)	$+42/+1/-16/-27$	$+45/+0/-16/-29$
C1 pure sources are SEQ and EQ only	holds	holds
C2 SEQ dominant out-hub, CF dominant in-hub	holds	holds
C3 critical network failure is a convergence node	holds	holds
C4 monotone four-layer cascade	holds	holds

4 Discussion

The marine seismic hazard chain condenses into a compact structure, in which a single class of triggers drives the cascade, a few hubs amplify it, and many consequence nodes absorb it. Marine and mainland earthquakes carry no incoming edges, and they reach most of the network within one or two steps, as the mean path lengths of 1.90 and 1.86 confirm. Because the cascade remains shallow, the window for interrupting it is short. Within this structure, the engineering-process layer holds the pivotal position, marking where natural hazards convert into technological failures and then propagate onward as socioeconomic loss. This study stresses that the gateway role rests on the layer's position, not on the sign of its net flow. At the fine 39-node resolution, this layer functions as a net sink, as diverse natural hazards independently trigger infrastructure and network failures. After aggregation into 15 hazard categories, these parallel input pathways are consolidated into unified links, thereby turning the layer into a weak net source. The two results remain consistent, and each holds at its own resolution. The change of sign reflects the loss of input diversity, not a change in mechanism. The resolution-invariant fact, therefore, is that the engineering layer sits at the natural-to-technological transition that defines a Natech coupling.

When compared at a common resolution, the marine and mainland chains share an identical four-layer architecture, but they differ in how they balance the flow. The mainland chain depends heavily on a single seismic source. Its out-degree centralisation reaches 0.832, and it routes a net inflow of about 45 % of all edges into the consequence layer, which together produce a concentrated, consequence-directed cascade. The marine chain, in contrast, distributes the flow more widely. Its triggering spreads across several secondary pathways, such as tsunamis and submarine landslides, its out-degree centralisation reaches only 0.551, and its higher network density of 0.271 lets the flow circulate laterally before settling. This study explains such structural contrasts from a physical mechanism perspective. Marine earthquakes can activate an extra hydrological branch represented by tsunamis, which diversifies secondary propagation pathways and disperses cascading risk loads. The contrast also orders the mitigation targets. Because neither the seismic sources nor the tsunamis they generate can be prevented, the

https://doi.org/10.5194/egusphere-2026-4167
Preprint. Discussion started: 9 September 2026

highest actionable leverage lies with the engineering hubs that carry the cascade, chiefly critical infrastructure failure and, once it is removed, fire; critical network failure is the convergence node that must be hardened, where the cascade accumulates. Node removal analysis quantifies the individual contribution of each node to cascading propagation. Network cascade reach is defined as the number of ordered hazard pairs connected by directed paths, calculated by summing the downstream hazards reachable from each individual hazard. The full 39-node network yields a total of 619 such ordered pairs. Deleting a node together with its edges, and recomputing the reach on the remainder, gives the share that the node carries. Critical infrastructure failure carries the most. Its removal lowers the reach by $34\,\%$, from 619 to 409 pairs, while the tsunami hub accounts for $14\,\%$ and critical network failure for $13\,\%$. A greedy search then assembles the most disruptive set one node at a time, adding at each step the node whose removal cuts the remaining reach the most and excluding the two uncontrollable seismic sources. It selects critical infrastructure failure, then fire, then the tsunami, and removing these three together lowers the reach by $61\,\%$, from 619 to 239 pairs. Fire outperforms critical network failure in propagation importance. When critical infrastructure failure is excluded from the network, fire dominates the remaining cascading pathways. Accordingly, this importance ranking captures the loss of directed reachability rather than relying solely on node degree. Since a single engineering node sustains approximately one-third of the entire cascading propagation, strengthening infrastructure and network layers provides substantially greater intervention efficacy than targeting individual natural hazards. This finding further validates the Natech transition gateway identified in Sect. 3.3 as the optimal intervention target. Moreover, the marine chain distributes its flow more widely than the mainland one, so marine mitigation cannot rely on protecting a single dominant pathway and must instead address several secondary branches in parallel.

The two analyses of this study also carry a general lesson for hazard-chain research. Degree-based topological metrics, including network density, centralisation and layer net flow, are sensitive to the taxonomic resolution of network construction. As demonstrated by the engineering-process layer in this work, a refined classification scheme can even reverse the apparent balance direction of layer net flow. Cross-network comparison therefore requires a common resolution, which this study adopts in Sect. 3.3, and resolution-dependent metrics should be reported with explicit caution. Several limitations nevertheless frame these results. The propagation model assumes independent events, pairwise interactions, and Markovian dynamics, so it simplifies the higher-order and memory effects seen in real cascades. The edges also remain binary and carry no triggering probability or time delay, so the network captures the structure of the couplings but not their strength or timing. The taxonomy and the encoding rest on expert judgement and on the documented tsunami record, which may under-represent rare pathways. Future work should therefore attach empirical triggering probabilities and delays to the edges, test the sensitivity of the conclusions to the encoding, and extend the framework towards a time-resolved description of cascade propagation.

5 Conclusions

This study models marine seismic hazard chains by combining catastrophe dynamics with graph theory. Using historical tsunami data, it builds a 39-node directed network and compares it with the mainland earthquake hazard chain. The marine hazard chain constitutes a shallow cascade structure consisting of one dominant source, two major hubs, and multiple sinks. Submarine and coastal earthquakes function as primary triggers, tsunamis and critical infrastructure failure act as key amplifying hubs, and critical network failure serves as the major convergence node. The engineering layer, in turn, works as a consistent Natech conversion gateway across resolutions. Under a unified taxonomic resolution, marine and mainland seismic hazard chains exhibit identical four-layer structural frameworks but distinct flow distribution patterns. The mainland hazard chain features strong centralisation and a pronounced tendency towards socioeconomic consequences, while the marine counterpart disperses risks through far more diversified secondary propagation pathways. These findings indicate that risk mitigation should target the controllable engineering hubs rather than the uncontrollable seismic sources, and that any cross-chain comparison requires a consistent taxonomic resolution.

Code and data availability. The secondary public datasets consulted in this study are openly available from PANGAEA (https://doi.pangaea.de/10.1594/PANGAEA.979839) and EM-DAT (https://public.emdat.be). The marine and mainland hazard-chain records (the documented cascade tables), the node lists and the 39-node and 15-class directed adjacency matrices, together with the R/`igraph` code that builds the networks and computes all reported metrics and figures, are available in the GitHub repository https://github.com/hazardchain/NHESS-marine-seismic-hazard-chains-code-data and are archived with a persistent DOI at Zenodo (version 1.0.1; https://doi.org/10.5281/zenodo.21316763, Shi et al., 2026).

Author contributions. YS conducted the quantitative analysis and drafted the original manuscript. CH performed the sensitivity analysis and cross-validation. ZZ carried out the investigation, reviewed and edited the manuscript, and supervised the study.

Competing interests. The contact author has declared that none of the authors has any competing interests.

Acknowledgements. We thank Arnaud Mignan for his initial support of this study. We thank reviewers for their comments, which helped improve this article. AI-based tools were used to assist with language editing and with the preparation of the reproducibility code; the authors reviewed and validated all content and take full responsibility for it.

Financial support. This work was supported by the National Key Research and Development Program of China (grant no. 2023YFC3008600), Shenzhen Science and Technology Program (grant no. JCYJ20241202125759001), the Guangdong Provincial Key Laboratory of Geophysical High-resolution Imaging Technology (grant no. 2022B1212010002), the Shenzhen Science and Technology Program (grant no. KQTD20170810111725321), the High Level Special Funds (grant no. G03050K001), and the National Natural Science Foundation of China (grant no. 42074054).

References

Alexander, D. and Pescaroli, G.: What are cascading disasters?, UCL Open Environment, p. e003, https://doi.org/10.14324/111.444/ucloe.000003, 2019.

Baltzopoulos, G., Cito, P., Ricci, F., Volpe, M., Selva, J., Cozzani, V., and Iervolino, I.: Earthquake and Tsunami NaTech Risk Assessment for Oil Storage Facilities, Earthquake Engineering & Structural Dynamics, 55, 1887–1904, https://doi.org/10.1002/eqe.70166, 2026.

Casas, G., Bastazini, V. A. G., Debastiani, V. J., and Pillar, V. D.: Assessing sampling sufficiency of network metrics using bootstrap, Ecological Complexity, 36, 268–275, https://doi.org/10.1016/j.ecocom.2018.09.005, 2018.

Chen, H., Ruan, H., Chen, J., Li, X., and Yu, Y.: Review of Investigations on Hazard Chains Triggered by River-Blocking Debris Flows and Dam-Break Floods, Frontiers in Earth Science, 10, 830 044, https://doi.org/10.3389/feart.2022.830044, 2022.

Efron, B. and Tibshirani, R. J.: An Introduction to the Bootstrap, Chapman & Hall/CRC, New York, 1993.

Fan, X., van Westen, C. J., Xu, Q., Gorum, T., and Dai, F.: Analysis of landslide dams induced by the 2008 Wenchuan earthquake, Journal of Asian Earth Sciences, 57, 25–37, https://doi.org/10.1016/j.jseaes.2012.06.002, 2012.

Fan, X., Fang, C., Dai, L., Wang, X., Luo, Y., Wei, T., and Wang, Y.: Near Real Time Prediction of Spatial Distribution Probability of Earthquake-induced Landslides — Take the Lushan Earthquake on June 1, 2022 as an Example, Journal of Engineering Geology, 30, 729–739, https://doi.org/10.13544/j.cnki.jeg.2022-0328, in Chinese, 2022.

Gill, J. C. and Malamud, B. D.: Reviewing and visualizing the interactions of natural hazards, Reviews of Geophysics, 52, 680–722, https://doi.org/10.1002/2013RG000445, 2014.

Gill, J. C. and Malamud, B. D.: Hazard interactions and interaction networks (cascades) within multi-hazard methodologies, Earth System Dynamics, 7, 659–679, https://doi.org/10.5194/esd-7-659-2016, 2016.

Han, L., Ma, Q., Zhang, F., Zhang, Y., Zhang, J., Bao, Y., and Zhao, J.: Risk Assessment of an Earthquake-Collapse-Landslide Disaster Chain by Bayesian Network and Newmark Models, International Journal of Environmental Research and Public Health, 16, 3330, https://doi.org/10.3390/ijerph16183330, 2019a.

Han, L., Zhang, J., Zhang, Y., Ma, Q., Alu, S., and Lang, Q.: Hazard Assessment of Earthquake Disaster Chains Based on a Bayesian Network Model and ArcGIS, ISPRS International Journal of Geo-Information, 8, 210, https://doi.org/10.3390/ijgi8050210, 2019b.

Helbing, D. and Kuehnert, C.: Assessing interaction networks with applications to catastrophe dynamics and disaster management, Physica A: Statistical Mechanics and its Applications, 328, 584–606, https://doi.org/10.1016/S0378-4371(03)00519-3, 2003.

Huang, F. L.: Using Cluster Bootstrapping to Analyze Nested Data with a Few Clusters, Educational and Psychological Measurement, 78, 297–318, https://doi.org/10.1177/0013164416678980, 2018.

Hüning, L. S. and Brunner, M. I.: Cascading impacts of natural disasters in a connected world, Science, 391, 1320–1322, https://doi.org/10.1126/science.adn8744, 2026.

Kabir, G., Suda, H., Cruz, A. M., Giraldo, F. M., and Tesfamariam, S.: Earthquake-related Natech risk assessment using a Bayesian belief network model, Structure and Infrastructure Engineering, 15, 725–739, https://doi.org/10.1080/15732479.2019.1569070, 2019.

Masuda, H., Sugawara, D., Cheng, A.-C., Suppasri, A., Shigihara, Y., Kure, S., and Imamura, F.: Modeling the 2024 Noto Peninsula earthquake tsunami: implications for tsunami sources in the eastern margin of the Japan Sea, Geoscience Letters, 11, 29, https://doi.org/10.1186/s40562-024-00344-8, 2024.

Mignan, A.: Introduction to Catastrophe Risk Modelling: A Physics-based Approach, Cambridge University Press, https://doi.org/10.1017/9781009437370, 2024.

https://doi.org/10.5194/egusphere-2026-4167
Preprint. Discussion started: 9 September 2026

Mignan, A. and Wang, Z.: Exploring the Space of Possibilities in Cascading Disasters with Catastrophe Dynamics, International Journal of Environmental Research and Public Health, 17, 7317, https://doi.org/10.3390/ijerph17197317, 2020.

Mignan, A., Mochel, L., and Ducos, G.: Involving Risk Reduction Practitioners and Other Experts in the Management of Super-Catastrophes via an Online Interactive Platform, Frontiers in Earth Science, 10, 829 145, https://doi.org/10.3389/feart.2022.829145, 2022a.

Mignan, A., Spada, M., Burgherr, P., Wang, Z., and Sornette, D.: Dynamics of severe accidents in the oil & gas energy sector derived from the authoritative ENergy-related severe accident database, PLoS ONE, 17, e0263 962, https://doi.org/10.1371/journal.pone.0263962, 2022b.

Norio, O., Ye, T., Kajitani, Y., Shi, P., and Tatano, H.: The 2011 eastern Japan great earthquake disaster: Overview and comments, International Journal of Disaster Risk Science, 2, 34–42, https://doi.org/10.1007/s13753-011-0004-9, 2011.

Park, J.-O., Mohammadigheymasi, H., Yamaguchi, A., Okino, K., Fujie, G., Jamali Hondori, E., Arikawa, T., Kurihara, T., and Imai, K.: Tsunamigenic fault structures revealed in the 2024 Noto earthquake (M7.6) rupture area, Scientific Reports, 16, 12 046, https://doi.org/10.1038/s41598-026-48075-4, 2026.

Pescaroli, G. and Alexander, D.: A definition of cascading disasters and cascading effects: Going beyond the "toppling dominos" metaphor, Planet@Risk, 3, 58–67, 2015.

Pescaroli, G. and Alexander, D.: Critical infrastructure, panarchies and the vulnerability paths of cascading disasters, Natural Hazards, 82, 175–192, https://doi.org/10.1007/s11069-016-2186-3, 2016.

Pescaroli, G. and Alexander, D.: Understanding Compound, Interconnected, Interacting, and Cascading Risks: A Holistic Framework, Risk Analysis, 38, 2245–2257, https://doi.org/10.1111/risa.13128, 2018.

Rocha, J. C., Peterson, G., Bodin, Ö., and Levin, S.: Cascading regime shifts within and across scales, Science, 362, 1379–1383, https://doi.org/10.1126/science.aat7850, 2018.

Shi, P., Ye, T., Wang, Y., Zhou, T., Xu, W., Du, J., Wang, J., Li, N., Huang, C., Liu, L., Chen, B., Su, Y., Fang, W., Wang, M., Hu, X., Wu, J., He, C., Zhang, Q., Ye, Q., and Okada, N.: Disaster Risk Science: A Geographical Perspective and a Research Framework, International Journal of Disaster Risk Science, 11, 426–440, https://doi.org/10.1007/s13753-020-00296-5, 2020.

Shi, Y., Hu, C., and Zhang, Z.: Code and data for: Quantitative Modelling of Marine Seismic Hazard Chains: Topology, Core Amplification Nodes, and Implications, https://doi.org/10.5281/zenodo.21316763, v1.0.1, 2026.

Somphong, C., Suppasri, A., Pakoksung, K., Nagasawa, T., Narita, Y., Tawatari, R., Iwai, S., Mabuchi, Y., Fujita, S., Moriguchi, S., Terada, K., Athanasius, C., and Imamura, F.: Submarine landslide source modeling using the 3D slope stability analysis method for the 2018 Palu, Sulawesi, tsunami, Natural Hazards and Earth System Sciences, 22, 891–907, https://doi.org/10.5194/nhess-22-891-2022, 2022.

Tacconi Stefanelli, C., Segoni, S., Casagli, N., and Catani, F.: Geomorphic indexing of landslide dams evolution, Engineering Geology, 208, 1–10, https://doi.org/10.1016/j.enggeo.2016.04.024, 2016.

Wang, F., Magoua, J. J., and Li, N.: Modeling cascading failure of interdependent critical infrastructure systems using HLA-based co-simulation, Automation in Construction, 133, 104 008, https://doi.org/10.1016/j.autcon.2021.104008, 2022.

Wang, J., Gu, X., and Huang, T.: Using Bayesian networks in analyzing powerful earthquake disaster chains, Natural Hazards, 68, 509–527, https://doi.org/10.1007/s11069-013-0631-0, 2013.

Xu, C., Xu, X., Yao, X., and Dai, F.: Three (nearly) complete inventories of landslides triggered by the May 12, 2008 Wenchuan Mw 7.9 earthquake of China and their spatial distribution statistical analysis, Landslides, 11, 441–461, https://doi.org/10.1007/s10346-013-0404-6, 2014a.

Xu, L., Meng, X., and Xu, X.: Natural hazard chain research in China: A review, Natural Hazards, 70, 1631–1659, https://doi.org/10.1007/s11069-013-0881-x, 2014b.

https://doi.org/10.5194/egusphere-2026-4167
Preprint. Discussion started: 9 September 2026

Yang, F.-Y., Zhuo, L., Xiao, M.-L., Xie, H.-Q., Liu, H.-Z., and He, J.-D.: A Statistical Risk Assessment Model of the Hazard Chain Induced by Landslides and Its Application to the Baige Landslide, Applied Sciences, 13, 3577, https://doi.org/10.3390/app13063577, 2023.

Yu, H., Wang, J., Chai, M., and Shi, P.: Review on research methods of disaster loss accumulation and amplification of disaster chains, Progress in Geography, 33, 1498–1511, https://doi.org/10.11820/dlkxjz.2014.11.007, in Chinese, 2014.

Yuhi, M., Umeda, S., Arita, M., Ninomiya, J., Gokon, H., Arikawa, T., Baba, T., Imamura, F., Kawai, A., Kumagai, K., Kure, S., Miyashita, T., Suppasri, A., Nobuoka, H., Shibayama, T., Koshimura, S., and Mori, N.: Post-event survey of the 2024 Noto Peninsula earthquake tsunami in Japan, Coastal Engineering Journal, 66, 405–418, https://doi.org/10.1080/21664250.2024.2368955, 2024.

Appendix A: Aggregation of the marine hazards into 15 common classes

To compare the marine and mainland chains at a common resolution (Sect. 3.3), this study aggregates the 39 marine hazard nodes into the same 15 classes used for the mainland chain. Table A1 lists the full node-to-class mapping; several merges are judgemental and hold under a broad water/geophysical reading, as noted below the table.

Table A1. Aggregation of the 39 marine hazard nodes into the 15 common hazard classes used for the marine–mainland comparison (Fig. 2, Table 4). Full peril names are given in Table 1.

Aggregated class	Abbr.	Constituent nodes*	Amount
Earthquake / trigger	EQ	SEQ, EQ, AS, VE	4
Mass slide	MS	SLS, CLS, LS, RO, LB, SA, LI, GU, SUB, MB	10
Critical infrastructure failure	CIF	CF, PHF, SDF, SPF, NFA	5
Critical network failure	CNF	NF, SCF	2
Fire	FI	FI, EX	2
Flood	FL	TS, CFL, FF	3
Water dilemma	WD	WP, WD	2
Flora and fauna	FA	FA, MED	2
Business interruption	BI	BI, MTD	2
Healthcare degradation	HD	HD, IR	2
Economic crisis	EC	EC	1
Disease	DI	DI	1
Physical and psychological trauma	PP	PP	1
Culture perils	CP	CP	1
Social unrest	SU	SU	1
Total			39

*Tsunami and fluvial flood join Flood; marine ecosystem damage joins Flora and fauna; maritime transport disruption joins Business interruption; insufficient rescue joins Healthcare degradation; and ground uplift, subsidence, liquefaction, and methane blowout join Mass slide.